Photoinduced and Dark Discharge Mechanisms of High Gamma Photoreceptors

Kuniki Seino, Hideaki Hirahara, Takaaki Konuma, Ichiro Yoshida and Shozo Kaieda

AFIT Corporation Hino, Tokyo 191-0016, Japan E-mail: seino@afit.co.jp

Abstract. An electrophotographic single-layer organic photoreceptor consisting of relatively low concentrations of phthalocyanine pigments dispersed in an insulating binder polymer, which is generally referred to as a high gamma photoreceptor, shows the induction effect. Several mechanisms have been proposed to explain this phenomenon. However it is not completely clear at this time. In this article, the photoinduced and dark discharge characteristics of the high gamma photoreceptors consisting of x-type metal-free phthalocyanine pigment and polyester polymer are found to be well described by a new theoretical model which takes into account structural trapping. We have found that good charge acceptance and high gamma characteristics depend on the presence of structural traps. © 2010 Society for Imaging Science and Technology.

[DOI: 10.2352/J.ImagingSci.Technol.2010.54.6.060502]

INTRODUCTION

Weigl reported in 1972 that an electrophotographic singlelayer organic photoreceptor consisting of relatively low concentrations of x-type metal-free phthalocyanine pigments dispersed in suitable binders exhibited a photodischarge induction effect¹ which was considered disadvantageous for analog copy machines. However, Kinoshita proposed in 1989 to use it as a digital light input photoreceptor.² Since then, photoreceptors with the induction effect have been referred to as "high gamma photoreceptors" where "gamma" refers to the slope of the photodischarge characteristics when plotted as surface potential vs. log (exposure). In 1991 Decker described a high gamma photoreceptor based on Kinoshita's idea.³ Although several mechanisms have been proposed to explain this unique phenomenon, 4-9 it is not completely clear at this time. In the present article, we present a theoretical model which takes into account the physical process of structural trapping is applied to not only the photoinduced but also the dark discharge characteristics of high gamma photoreceptors. We have found that desirable electrophotographic performance characteristics such as good charge acceptance, low dark decay rate, and high gamma depend on structural traps.

Received Jan. 11, 2010; accepted for publication Jul. 19, 2010; published online Nov. 5, 2010.

1062-3701/2010/54(6)/060502/9/\$20.00.

EXPERIMENTAL

A high gamma photoreceptor with x-type metal-free pthalocyanine pigments dispersed in polyester binder was investigated (Digital Photoreceptor HGPC). Hardness and moisture-fastness of the binder are improved by cross-linking to a low molecular weight polyester (about 5000) using butylated melamine resin.

The formulation comprised the following:

- (1) Polyester resin (Almatex[™] P645 by Mitsui Chemical) 40 g (60% solids).
- (2) Butylated melamine resin (U-van[™] 20HS by Mitsui Chemicals) 7 g (70% solids).
- (3) Cyclohexanone (first grade chemical reagent) 150 g.
- (4) Metal-free phthalocyanine pigment resin (Fastgen™ Blue 8120BS by Dainippon Ink and Chemicals) 9.6 g.

Chemicals 1, 2, and 3 were placed in a glass bottle (450 ml) and stirred until dissolved. The pigment was added with 200 g glass beads (3 mm diameter) followed by 4 h shaking. Then the mixture was filtered to prepare the coating dispersion. The viscosity was 500 m Pa·s. An aluminum foil (80 μ m thickness) was taped to an Al tube and ring coated with the dispersion at the rate of 200 mm/min. The coating was air dried at 150 °C for 1 h. The dried coating was about 18 μ m in thickness and the average diameter of the pthalocyanine pigment particles was measured to be 0.7 μ m (Horiba LB-550 Dynamic Light Scattering Nanoparticle Size Analysis System). The specific gravity of the pthalocyanine pigment is 1.44 and that of binder is 1.2, therefore the binder content is 78.3 vol % (75.0 wt %) and pthalocyanine content is 21.7 vol % (25.0 wt %).

The photoinduced and dark discharge characteristics of Digital Photoreceptor HGPC were measured by the conventional method to obtain the photoinduced discharge curve (PIDC). A schematic of the experimental arrangement is illustrated in Figure 1. The photoconductive drum was corona charged and then exposed to monochromatic light (710 nm from a halogen lamp with interference filters monitored by an Hioki Optical Power Meter 3664). The exposure was initiated and stopped by a shutter between the lamp and the optical fiber. The exposure slit was 0.2 mm. The diameter of the photoconductive drum was 80 mm and the circumferential velocity 55.85 mm/s giving an exposure time of 3.6

IS&T member

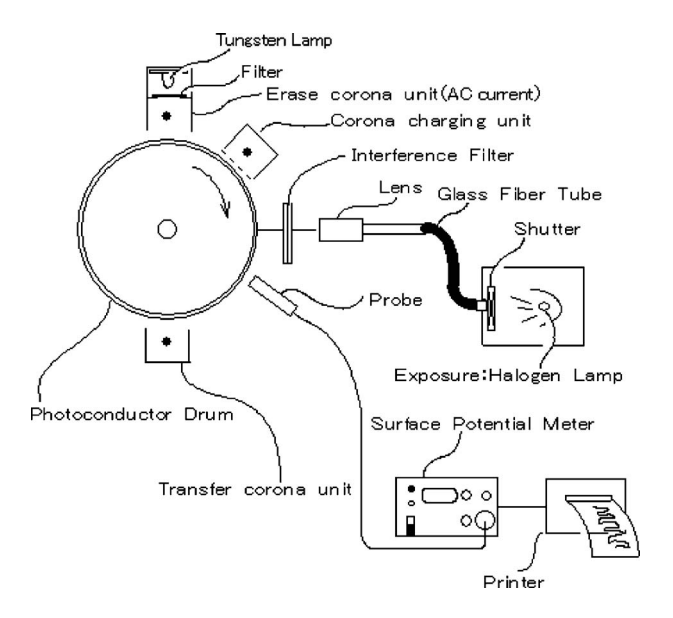


Figure 1. Experimental arrangement for measuring photoinduced and dark discharge characteristics. Wavelength of exposure is 710 nm; exposure time is 3.6 ms, and time between exposure and probe is 0.3 s.

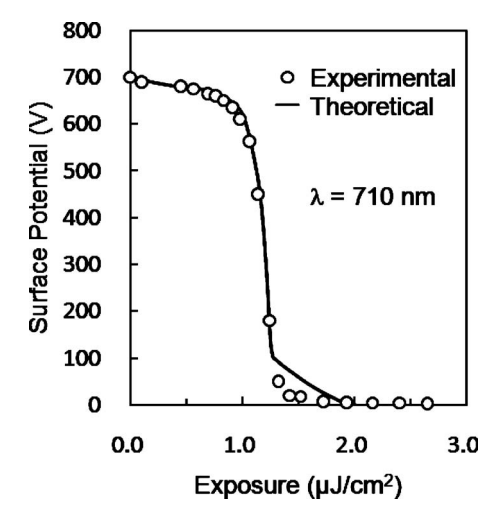


Figure 2. Photoinduced discharge characteristics for the Digital Photoreceptor HGPC. Exposure time is 3.6 ms with light of 710 nm. The theoretical curve is calculated with $d_{\rm s}{=}0.02~\mu{\rm m}$, $N_{\rm l}{=}15$ layers, and $\eta_0{=}0.88$. The details of the theoretical calculation are described in the text.

ms. The exposure intensity was controlled by changing the supply voltage of the light source. The surface potential of the photoconductive drum was measured 0.3 s after the exposure. To stabilize the photoinduced and dark discharge characteristics, simultaneous AC corona charging and erase exposures were used.

RESULTS

The surface potential was measured as the photoconductive drum rotated and the supply voltage to the halogen lamp was changed stepwise after each complete rotation. The measured surface potentials were plotted as a function of the exposure, the dark discharge characteristics were measured every rotation of the photoconductive drum after the expo-

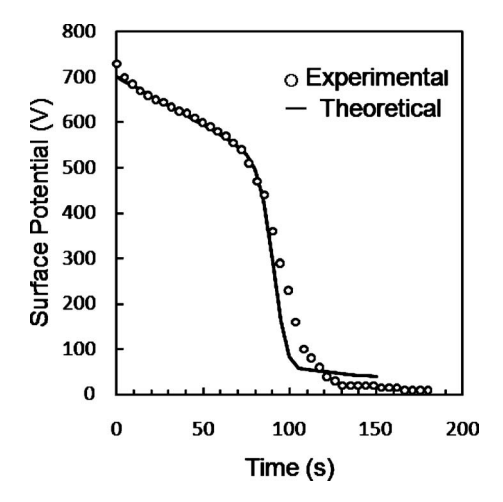


Figure 3. Dark discharge characteristics for the Digital Photoreceptor HGPC. The theoretical curve is calculated with d_s =0.02 μ m, N_L =15 layers, and G=4.2 \times 10¹³ cm⁻³ s⁻¹. The details of the theoretical calculation are described in the text.

sure was shut off. The photoinduced discharge characteristics at 710 nm for the positively charged Digital Photoreceptor HGPC are shown in Figure 2. The photodischarged surface potential decreases rapidly after a threshold exposure; (Weigl has referred to this as the induction exposure¹). The observed threshold exposure is about 1.1 μ J/cm². In the case of negative charging, little discharge is observed even for the exposure of 1.7 μ J/cm². This result suggests that hole-electron pairs are photogenerated in a narrow region close to the charged surface (less than 0.1 μ m) and electrons are immobile.

The experimental results for dark discharge of Digital Photoreceptor HGPC are shown in Figure 3. The observed dark decay rate is initially slow, about 2.5 V/s; however after about 80 s the surface potential decays rapidly.

DISCUSSION Structural Trap Model

The high gamma photoreceptor consists of relatively low concentrations of pthalocyanine pigments dispersed in an insulating binder polymer. However the residual potential of Digital Photoreceptor HGPC is low as shown in Fig. 2. This means that carrier transport paths through the film are efficiently formed in spite of a low concentration of photoconductive particles. Kitamura has determined experimentally that the phthalocyanine pigments form endless chains in the layer at pigment concentrations higher than 20 wt %.6 Phthalocyanine pigments are dissolved by dipping the layer into a sulfuric acid solution. He concluded that the phthalocyanine pigments were in contact with each other because the sulfuric acid solution could penetrate through the layer. According to percolation theory, endless conducting chains are formed at concentrations higher than 16 vol % of random close packed mixtures of conducting and insulating spheres and the average number of contact points is 2.1.

Figure 4(a) gives a schematic view of formation of the endless chain described above. As is indicated schematically, under such circumstances the contact point of a particle

Structural trap

Structural trap model

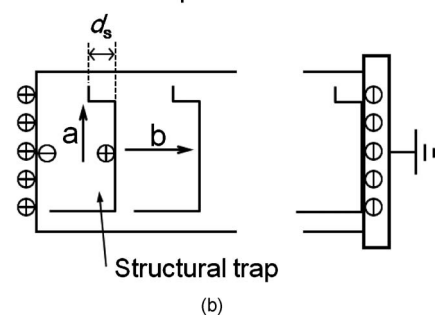


Figure 4. (a) A schematic view for structural traps produced by random contact between photoconductive particles dispersed in an insulating binder polymer. The arrows $\bf a$ and $\bf b$ indicate the direction of hole movement. (b) A structural trap model with structural trap depth $d_{\rm s}$ for a high gamma photoreceptor.

with an adjacent particle can be offset from the center of the base of the spherical bodies in the direction of the electric field. In this case free carriers (holes) are considered to be trapped within the saucer-shaped-space surrounded by insulating binder polymer. ^{9,10} We call this a structural trap. The physical depth of the structural trap is shown. In some subsequent figures the physical trap depth will also be used to represent the energetic trap depth.

In the case of strong light absorption, hole-electron pairs are photogenerated in a narrow region close to the surface, and free holes are trapped in the first structural trap under a strong electric field due to surface charges. Electron space charges close to the surface increase with exposure time, the electric field in the first structural trap decreases. Finally trapped holes begin to detrap at the particle-to-particle contact point indicated by an arrow **a**. The detrapped holes are transported in the particle indicated by the arrow **b**.

Figure 4(b) shows the structural trap model for theoretical calculations corresponding to Fig. 4(a), where d_s is the average structural trap depth and structural trap layers are assumed to be distributed evenly at an average distance.

Energy Barrier of Structural Traps

Figure 5 shows a generalized structural trap model, where d_s is the structural trap depth, $\Phi_{\rm B}$ is the energy barrier for hole detrapping, $E_{\rm c}$ is the electric field due to the surface charges n_0 (cm⁻²), the concentration of photogenerated trapped electrons $n_{\rm g}$ (cm⁻²) and holes outside of the structural trap, and $n_{\rm t}$ (cm⁻²) is the concentration of trapped holes.

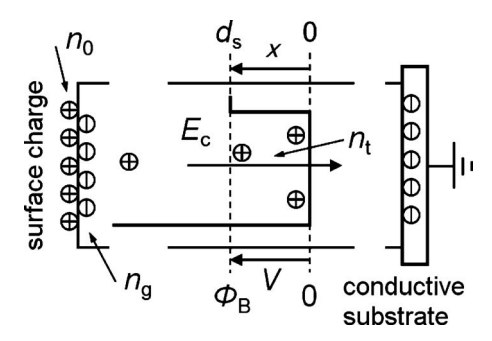


Figure 5. A generalized structural trap model with energy barrier Φ_{B} in a photoconductive layer of the high gamma photoreceptor. The symbols are described in the text.

The electric field E_0 at the bottom of the structural trap (x=0) is related to the electric field E_c and the trapped holes n_t by Gauss's law as follows:

$$E_0 = E_c + e n_t / \varepsilon_r \varepsilon_0, \tag{1}$$

where e is the electronic unit of charge, ε_r the relative permittivity and ε_0 the permittivity of vacuum. The increment of potential ΔV_1 at the distance of $x = \Delta x$ from the bottom is given by

$$\Delta V_1 = E_0 \Delta x = (E_c + e n_t / \varepsilon_r \varepsilon_0) \Delta x. \tag{2}$$

Therefore the potential V_1 at the distance of $x_1(=\Delta x)$ from the bottom is given by

$$V_1 = \Delta V_1. \tag{3}$$

The distribution function of electrons and holes in thermal equlibrium is the Fermi-Dirac distribution. In our analysis we use the Maxwell-Boltzmann distribution, a commonly used approximation if the barrier height is much larger than kT. The Maxwell-Boltzmann distribution f(v) is applied to trapped holes as follows:

$$f(v)dv = \left(\frac{m}{2\pi kT}\right)^{0.5} \exp\left(-\frac{mv^2}{2kT}\right) dv,\tag{4}$$

where ν is the velocity of holes, m the hole mass, k the Bolzmann constant, and T the absolute temperature in Kelvin. Assuming that the contact points to the next photoconductive particle are close to 1 as shown in Fig. 4, unidirectional charge motion in one dimension is taken into account in Fig. 5. A function $F(\nu)$ is defined by integrating Eq. (4) with respect to ν from ν to $+\infty$.

$$F(v) = \int_{v}^{+\infty} f(v)dv.$$
 (5)

In the case of v = 0, F(0) = 0.5.

The kinetic energy of holes at the distance x_1 equals the potential V_1 obtained from Eq. (3). Then the velocity of holes at x_1 is given by

$$v_1 = (2eV_1/m)^{0.5}. (6a)$$

The general expression is as follows:

$$v_N = (2eV_N/m)^{0.5}$$
. (6b)

Then, $F(v_1)$ is given by

$$F(\nu_1) = 0.5 - f(0) \cdot \Delta \nu_1. \tag{7a}$$

The general expression is as follows:

$$F(\nu_N) = F(\nu_{N-1}) - f(\nu_{N-1}) \cdot (\nu_N - \nu_{N-1}), \quad (N \ge 1).$$
(7b)

In the case of N=1, $v_{N-1}=0$, and $2F(v_{N-1})=1$.

The potential V_2 at the distance of $x=x_1+\Delta x$ is given by using $F(v_1)$ as follows:

$$V_2 = V_1 + (E_c + 2en_t F(v_1)/\varepsilon_r \varepsilon_0) \Delta x. \tag{8a}$$

The general expression is as follows:

$$V_N = V_{N-1} + (E_c + 2en_t F(\nu_{N-1})/\varepsilon_r \varepsilon_0) \Delta x.$$
 (8b)

The energy barrier $\Phi_{\rm B}$ can be obtained by successive calcuration from x=0 to $d_{\rm s}$.

Detrapping Rates from Structural Traps

The kinetic energy of holes equal to the energy barrier Φ_{B} is expressed as

0.5 m
$$v_0^2 = \Phi_B$$
, (9)

$$v_0 = (2\Phi_{\rm B}/m)^{0.5}. (10)$$

The hole density Δn with respect to ν from ν to $\nu + \Delta \nu$ is

$$\Delta n = n_t f(v) \Delta v. \tag{11}$$

Therefore, hole flux from the structural trap becomes

$$dj = v\Delta n = v n_t f(v) \Delta v. \tag{12}$$

The detrapping rate of trapped holes is obtained by integrating Eq. (12) with respect to ν from ν_0 to $+\infty$. This leads to the following equation:

$$\frac{dn_{\rm dt}}{dt} = -n_t \left(\frac{kT}{2\pi m}\right)^{0.5} \exp\left(-\frac{\Phi_{\rm B}}{kT}\right). \tag{13}$$

Photoinduced Discharge Mechanism

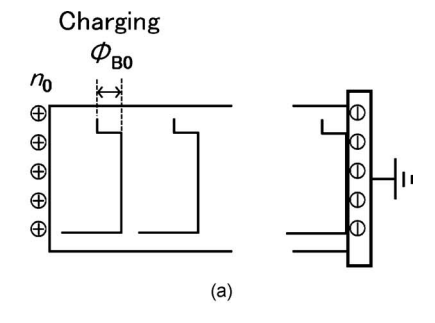
The photoinduced discharge mechanism for high gamma photoreceptors is schematically illustrated in Figure 6. The structural trap layers with the energy barrier Φ_B are distributed periodically at an average distance.

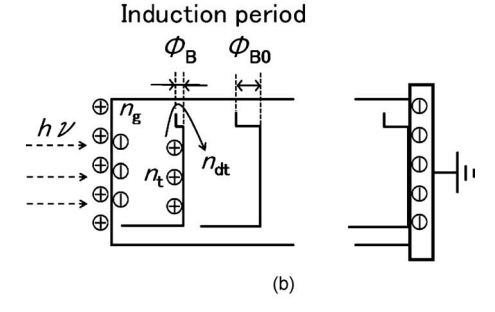
The initial surface potential V_0 with positive corona charging is defined as follows:

$$V_0 = e n_0 d_{\rm p} / \varepsilon_r \varepsilon_0, \tag{14}$$

where $d_{\rm p}$ is the layer thickness and n_0 is the surface charge density. The initial energy barrier $\Phi_{\rm B0}$ shown in Fig. 6(a) is related to the initial surface potential V_0 by the equation

$$\Phi_{\rm B0} = V_0 d_{\rm s} / d_{\rm p}. \tag{15}$$





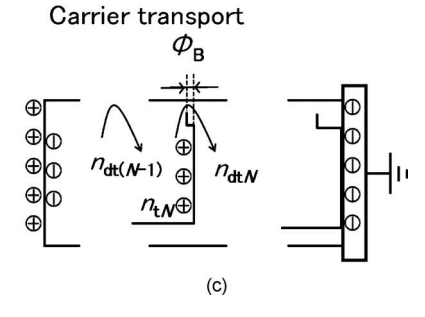


Figure 6. Photoinduced discharge mechanism for a high gamma photoreceptor based on the structural strap model. The symbols are described in the text.

In the case of strong light absorption, hole-electron pairs are photogenerated in a narrow region close to the charged surface as shown in Fig. 6(b).

The quantum efficiency of the field-controlled carrier photogeneration in x-type metal-free phthalocyanine is reported by Hackett¹³ as follows:

$$\eta(E) = \exp[(\beta_{pf} E^{0.5} / kT) - (\Phi_{0pf} / kT)],$$
(16)

where E is the electric field, and $\beta_{pf}=1.06\times10^{-4}$ eV cm^{0.5} V^{-0.5}, $\Phi_{0pf}=0.09$ eV for a wavelength of 620 nm.¹³ A correction factor η_0 is added to Hackett's equation in consideration of the difference in wavelengths and sample preparation.

$$\eta(E) = \eta_0 \exp[(\beta_{pf} E^{0.5}/kT) - (\Phi_{0pf}/kT)].$$
(17)

The photogeneration rate for hole-electron pairs n_g can be expressed as

$$dn_{\sigma}/dt = F \eta(E), \tag{18}$$

where F is the exposure light intensity in photons cm⁻² s⁻¹. Then

$$n_{\rm g}(t) = \int dn_{\rm g}. \tag{19}$$

As shown in Fig. 6(b), the photogenerated holes are trapped in the first structural trap layer close to the photoconductive surface. Assuming that carrier transit time in photoconductive particles is short, the photoinduced discharge time is determined by the time required for trapping and detrapping.

The energy barrier of the first structural trap layer decreases with exposure time, and finally the trapped holes begin to detrap to the second structural trap layer. The detrapping rate of trapped holes is obtained by Eq. (13) in which $E_{\rm c}$ is given by

$$E_{c} = e[n_{0} - n_{g}(t)]/\varepsilon_{r}\varepsilon_{0}. \tag{20}$$

Then, the time dependence for hole detrapping can be obtained by

$$n_{\rm dt}(t) = \int dn_{\rm dt}.$$
 (21)

The instantaneous concentration of trapped holes $n_t(t)$ in the first structural trap is given by

$$n_{\rm t}(t) = n_{\rm g}(t) - n_{\rm dt}(t)$$
. (22)

The structural trap situation within the photoconductive layer during the carrier transport process is shown in Fig. 6(c). The detrapping rate for trapped holes with $N \ge 2$ is obtained from Eq. (13) in which E_c is given by

$$E_{c} = e(n_{0} - n_{tN} - n_{dtN})/\varepsilon_{r}\varepsilon_{0}.$$
(23)

Then, the detrapped holes concentrations can be obtained by

$$n_{\rm dtN}(t) = \int dn_{\rm dtN}.$$
 (24)

The trapped hole concentration in the Nth structural trap layer n_{tN} is determined as follows:

$$n_{tN}(t) = n_{dt(N-1)}(t) - n_{dtN}(t).$$
 (25)

Therefore, the potential V_{tN} due to the trapped holes at the Nth structural trap layer is given by

$$V_{tN}(t) = e n_{tN}(t) d_{p}(1 - N/N_{L}) / \varepsilon_{r} \varepsilon_{0}, \qquad (26)$$

where $N_{\rm L}$ is number of structural trap layers in the photoconductor. Therefore, the instantaneous surface potential of the photoconductive layer $V_{\rm s}(t)$ is calculated using Eqs. (19) and (26) is as follows:

$$V_{s}(t) = V_{0} - \frac{e n_{g}(t) d_{p}}{\varepsilon_{s} \varepsilon_{0}} + \sum_{N=1}^{N_{L}} V_{tN}(t),$$
 (27)

where $n_{t1}(t)$ and $n_{tN}(t)(N \ge 2)$ in Eq. (26) can be obtained by successive calculation from Eqs. (17)–(22) and Eqs. (23)–(25), respectively.

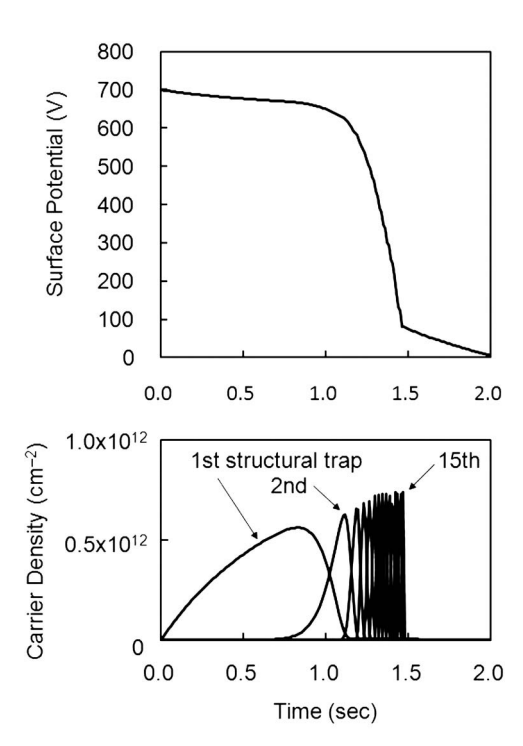


Figure 7. Carrier transport mechanism and surface potential decay for continuous exposure with low light intensity. Light intensity is $1~\mu W/cm^2$ and layer thickness is $1.8~\mu m$. The theoretical curves are calculated with $d_{\rm s}{=}0.02~\mu m$, $N_{\rm l}{=}15$ layers and $\eta_{\rm 0}{=}0.88$.

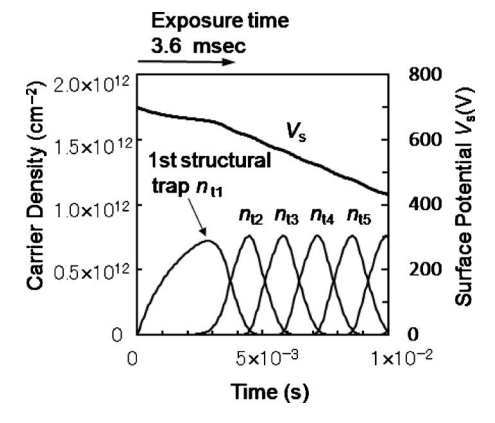


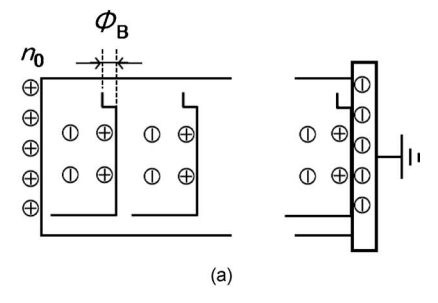
Figure 8. Carrier transport mechanism and surface potential decay calculated for an exposure time of 3.6 ms and light intensity of 472 μ W/cm² (the exposure is 1.7 μ J/cm²). Layer thickness is 1.8 μ m. The theoretical curve is calculated with d_s =0.02 μ m, N_l =1.5 layers, and η_0 =0.88.

The photoinduced discharge mechanism for continuous exposure with low light intensity is shown in Figure 7. The surface potential is plotted as a function of exposure time

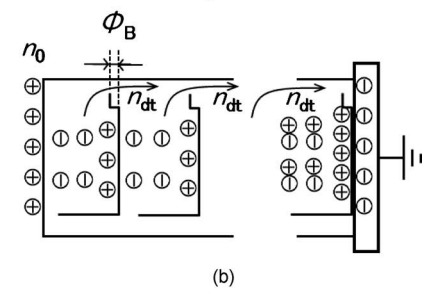
calculated with an initial surface potential V_0 =700 V, layer thickness $d_{\rm p}$ =18 μ m, relative permittivity $\varepsilon_{\rm r}$ =4, temperature T=298 K, wavelength λ =710 nm, exposure light intensity F=1 μ W/cm², structural trap depth $d_{\rm s}$ =0.02 μ m, the total number of structural trap layers $N_{\rm L}$ =15 layers and the correction factor η_0 =0.88.

The photoinduced discharge curve in Fig. 7 shows the typical induction effect. The hole density in the first struc-

Slow dark decay period



Fast dark decay



Charge distribution in the layer

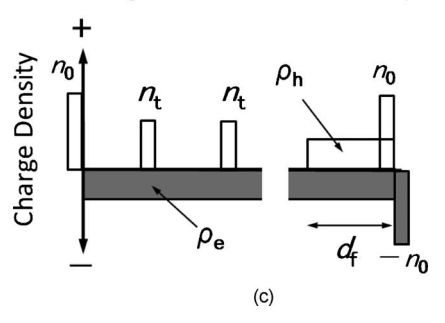


Figure 9. The dark discharge mechanism for a high gamma photoreceptor based on the structural trap model.

tural trap increases with exposure time and detrapping occurs to the second structural trap. Holes are transported to the next structural trap one after another. After the group of

holes reaches the conducive substrate, the surface potential decay rate is limited by the carrier photogeneration rate.

Figure 8 shows the photoinduced discharge mechanism for a short time exposure calculated with an initial surface potential V_0 =700 V, layer thickness d_p =18 μ m, relative permittivity $\varepsilon_r = 4$, temperature T = 298 K, wavelength λ=710 nm, exposure time=3.6 ms, exposure light intensity $F=472 \mu \text{W/cm}^2$ (exposure=1.7 $\mu \text{J/cm}^2$), structural trap depth d_s =0.02 μ m, the total number of structural trap layers $N_L = 15$ layers and the correction factor $\eta_0 = 0.88$. The hole density in the first structural trap increases with exposure time and detrapping occurs to the second structural trap. After the exposure, holes are transported to the next structural trap one after another, and finally reach the conductive substrate. In this case it takes 20 ms. The surface potential V_s decays in proportion to the transport distance of the group of holes from the surface and reaches a final potential of 29 V. This example is the "Theoritical"

photodischarge curve shown in Fig. 2 where the final potential (V_s) is 29 V and the exposure is 1.7 μ J/cm².

Dark Discharge Mechanism

The dark discharge mechanism for high gamma photoreceptors based on our structral trap model is schematically illustrated in Figure 9.

Holes and electrons are thermally generated in all regions of the photoconductive layer as shown in Fig. 9(a). The thermal carrier generation rate can be expressed as

$$dn_{\rm g}/dt = Gd_{\rm p}/N_{\rm L},\tag{28}$$

where $d_{\rm p}$ is the layer thickness, $N_{\rm L}$ is the total number of structural trap layers, and G (cm⁻³ s⁻¹) is the thermal carrier generation efficiency. Then the concentration of thermally generated hole-electron pairs is given by

$$n_{g}(t) = Gd_{p}t/N_{L}. \tag{29}$$

Electrons in x-type metal-free pthalocyanine pigment are immobile so the electron space charge density $\rho_{\rm e}(t)$ (C cm⁻³) is given by

$$\rho_e(t) = e n_o(t) N_{\rm I} / d_{\rm p}. \tag{30}$$

Then the negative potential $V_{\rm e}$ due to the electron space charge is obtained by

$$V_{\rm e}(t) = d_{\rm p}^2 \rho_{\rm e}(t) / 2\varepsilon_r \varepsilon_0. \tag{31}$$

The thermally generated free holes are trapped in the structural trap layers as shown in Fig. 9(a). Assuming that the carrier transit time in the photoconductive particles is short, the dark discharge rate is determined by the time required for trapping and detrapping.

The surface potential due to trapped holes at the *N*th structural trap numbered from the conductive substrate is given by

$$V_{tN} = e n_t(t) d_p N / \varepsilon_r \varepsilon_0 N_L, \qquad (32)$$

where the structural trap in contact with the conductive substrate is not counted because it is considered to be at zero potential. The potential $V_{\rm t}(t)$ due to the holes $n_{\rm t}(t)$ trapped by the structural traps from the 1st to the $N_{\rm L}-1$ -th layer is given by

$$V_{t}(t) = \frac{en_{t}(t)d_{p}}{\varepsilon_{r}\varepsilon_{0}N_{L}} \sum_{N=1}^{N_{L}-1} N = \frac{en_{t}(t)d_{p}(N_{L}-1)}{2\varepsilon_{r}\varepsilon_{0}}.$$
 (33)

As the dark discharge proceeds, polarization between the immobile electron space charge and trapped free holes increases, the energy barriers for all of the structural trap layers decrease, and then finally trapped holes begin to detrap. We assume for convenience that all trapped holes detrap together.

The detrapping rate of trapped holes is obtained by Eq. (13) in which E_c is given by

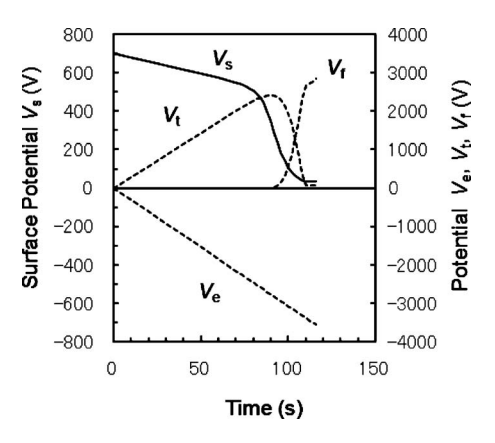


Figure 10. The dark discharge mechanism for high gamma photoreceptors. The theoretical curves are calculated with d_p =18 μ m, d_s =0.02 μ m, N_L =15 layers. The symbols are described in the text.

$$E_c = e(n_0 - n_\sigma)/\varepsilon_r \varepsilon_0. \tag{34}$$

Then, the time dependence for hole detrapping holes $n_{\rm dt}(t)$ can be obtained by

$$n_{\rm dt}(t) = \int dn_{\rm dt}.$$
 (35)

The instantaneous trapped hole concentration $n_t(t)$ can be expressed as follows:

$$n_{\rm t}(t) = n_{\rm g}(t) - n_{\rm dt}(t)$$
. (36)

It is assumed that the detrapped holes transport without subsequent trapping or recombination. As shown in Fig. 9(b), detrapped holes neutralize the charges on the conductive substrate as follows:

$$n_0 = n_t(t) + n_{dt}(t) + n_{dt}(t)(N_1 - 1),$$
 (37)

where $n_{\rm t}(t)$ and $n_{\rm dt}(t)$ are the trapped and the detrapped holes relative to the structural trap in contact with the conductive substrate. $n_{\rm dt}(t)(N_{\rm L}-1)$ is the time dependent number of detrapped holes that reach the conductive substrate.

As shown in Fig. 9(c), successively the detrapped holes neutralize the electron space charge. The space charge neutralization boundary, $d_{\rm f}$ is given by

$$n_{\rm g}(t)(N_{\rm L}/d_{\rm p})d_{\rm f} = n_{\rm dt}(t)(N_{\rm L} - 1) - \left[n_0 - n_{\rm t}(t) - n_{\rm dt}(t)\right] + \left[n_{\rm t}(t)(N_{\rm L} - 1)/d_{\rm p}\right]d_{\rm f}. \tag{38}$$

Then, Eq. (38) becomes

$$d_{\rm f}(t) = \frac{n_{\rm dt}(t)(N_{\rm L} - 1) - \left[n_0 - n_{\rm t}(t) - n_{\rm dt}(t)\right]}{n_{\rm g}(t)N_{\rm L}/d_{\rm p} - n_{\rm t}(t)(N_{\rm L} - 1)/d_{\rm p}}.$$
 (39)

The hole space charge density $\rho_{\rm h}({\rm C~cm^{-3}})$ at the neutralized region

$$\rho_{\rm h}(t) = e\{n_{\rm dt}(t)(N_{\rm L} - 1) - [n_0 - n_{\rm t}(t) - n_{\rm dt}(t)]\}/d_{\rm f}(t). \tag{40}$$

The potential due to hole space charge $V_f(t)$ is given by

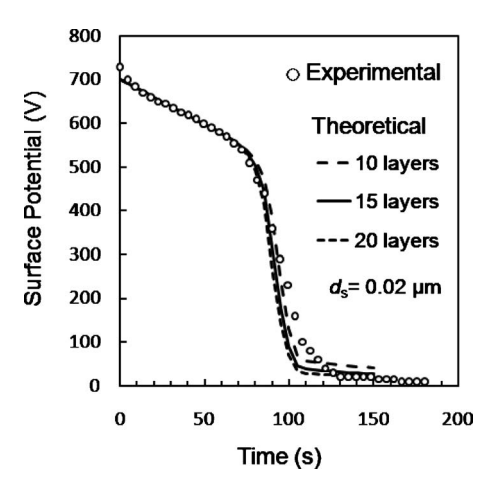


Figure 11. Dark discharge characteristics calculated with varying numbers of structural trap layers. The structural trap depth is determined to be $d_{\rm s}{=}0.02~\mu{\rm m}$ and $G/N_{\rm l}{=}2.8{\times}10^{12}~{\rm cm}^{-3}~{\rm s}^{-1}$.

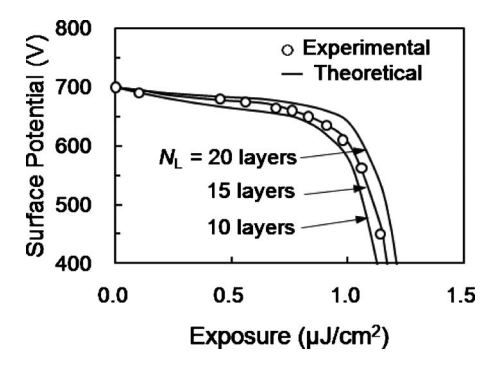


Figure 12. Photoinduced discharge chracteristics for Digital Photoreceptor HGPC. The number of structural trap layers $N_{\rm l}$ is determined to be 15 layers and the quantum efficiency correction factor (η_0) is 0.88.

$$V_{\rm f}(t) = d_{\rm f}(t)^2 \rho_{\rm h}(t) / 2\varepsilon_r \varepsilon_0. \tag{41}$$

The surface potential of the photoconductive layer $V_s(t)$ can be obtained by

$$V_{s}(t) = V_{0} - V_{e}(t) + V_{t}(t) + V_{f}(t), \tag{42}$$

where $V_e(t)$, $V_t(t)$, and $V_f(t)$ are obtained by successive calculation from Eqs. (28)–(31), Eqs. (32) and (33), and Eqs. (34)–(41), respectively.

Figure 10 shows an example calculated with an initial surface potential V_0 =700 V, layer thickness $d_{\rm p}$ =18 μ m, relative permittivity $\varepsilon_{\rm r}$ =4, temperature T=298 K, structural trap depth $d_{\rm s}$ =0.02 μ m, and the total number of structural trap layers $N_{\rm L}$ =15 layers.

Methods for Estimating Structural Trap Depth (d_s) and the Number of Structural Trap Layers (N_L)

The theoretical dark discharge curves shown in Figure 11 were calculated using the method of successive calculation with Eqs. (28)–(42) varying the number of structural trap layers, where layer thickness $d_{\rm p}$ =18 μ m, initial surface potential V_0 =700 V, relative permittivity $\varepsilon_{\rm r}$ =4, temperature

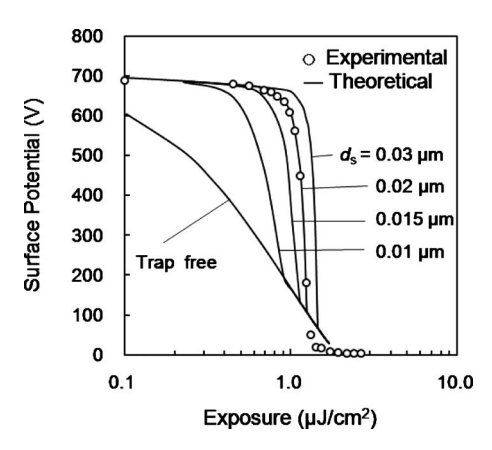


Figure 13. Photodischarge characteristics of high gamma photoreceptors simulated with various structural trap depths.

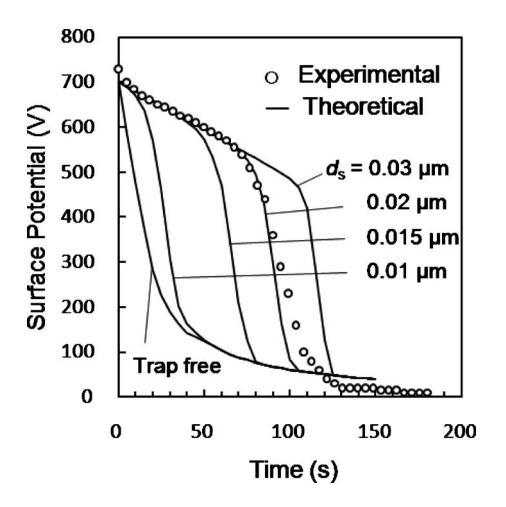


Figure 14. Dark discharge characteristics for the high gamma photoreceptors simulated with various structural trap depths.

T=298 K and $G/N_{\rm L}$ =2.8 \times 10¹² cm⁻³ s⁻¹. The calculated structural trap depth $d_{\rm s}$ is 0.02 μ m.

The theoretical photoinduced discharge curves shown in Figure 12 were calculated using the method of successive calculation by Eqs. (14)–(27). The correction factor for the quantum efficiency (η_0) is 0.88. As shown in Fig. 12, the number of structural trap layers $N_{\rm L}$ is calculated to be 15 layers for a photoconductor thickness of 18 μ m. This means that the average distance between structural trap layers is 1.2 μ m.

Figs. 2 and 3 show the theoretical photoinduced and dark discharge curves calculated using $d_{\rm s}$ =0.02 μ m and $N_{\rm L}$ =15 layers as described above.

ELECTROPHOTOGRAPIC PERFORMANCE

It has been shown that high gamma photoreceptors can sharpen the edges of electrostatic latent images in a laser printer and create hardcopies printed with high resolution and high quality.^{3,4} Konuma reported that the Digital Photoreceptor HGPC achieved high resolution images when developed with liquid toner.¹⁴

Photoinduced discharge curves for Digital Photoreceptor HGPC are shown with a logarithmic exposure scale in

Figure 13 along with photodicharge curves simulated for various structural trap depths.

The dark decay rate can be obtained by from Eqs. (31) and (33) as follows:

$$\frac{dV_{\rm s}}{dt} = \frac{dV_{\rm e}}{dt} - \frac{dV_{\rm t}}{dt} = -\frac{ed_{\rm p}^2 G}{2\varepsilon_{\rm r} \varepsilon_0 N_{\rm L}}.$$
 (43)

The dark decay rate for a trap free photoreceptor has been described by Eq. (43) with $N_{\rm L}{=}1$. Therefore the dark decay rates of high gamma photoreceptors are improved with increasing $N_{\rm L}$. It has been reported that the thermal generation rates of single-layer photoreceptors are substantially higher than dual layer photoreceptors. However, it is found theoretically that a slow dark decay rate in a high gamma photoreceptors depends on the limited displacement within $d_{\rm p}/N_{\rm L}$ for thermally generated holes. Figure 14 shows the dark dicharge curves simulated with various structural trap depths. The time dependence of the slow dark decay period depends on the structural trap depth.

The time for the trapping and detrapping processes during carrier transport is calculated to be 20×10^{-3} s at the exposure of 1.7 μ J/cm² as shown in Fig. 8. This is significantly shorter than the typical time between exposure and development (about 0.1–0.3 s). Thus, in spite of charge carrier trapping during carrier transport, the photoresponse time for the x-type metal-free phthalocyanine OPC is consistent with high resolution digital imaging.

CONCLUSION

The photoinduced and dark discharge mechanisms of high gamma photoreceptors are clarified by a new theoretical model which takes into account the physical process of structural trapping. New methods for estimating structural trap depths and the distance between structural traps are developed.

It is necessary to reconsider methods for measuring photoinduced discharge characteristics. Photoinduced and dark decay discharge should be measured in parallel to investigate the importance of structural trapping. The dark discharge is not due to carrier leakage but electrostatic polarization in the pigment particles. The transit time measured by the time-of-flight method depends on carrier transport in a particle and trapping by a structural trap. The latter is estimated by our new theoretical model.

We have shown that structural traps create a complex electrostatic latent image formation mechanism. The photoconductive layer becomes a dielectric insulator after corona charging, however, after the induction exposure the photoconductive layer becomes charge transporting. High gamma characteristics enable these characteristics. The high gamma photoreceptor has good charge acceptance, low dark decay rate, high gamma, and fast photoresponse.

ACKNOWLEDGMENT

The authors would like to thank Dr. Inan Chen for valuable discussions. The authors would like to thank Dr. David S.

Weiss who reviewed this article and provided valuable suggestions.

REFERENCES

- ¹ J. W. Weigl, J. Mammino, G. L. Whittaker, R. W. Radler, and J. F. Byrne, *Current Problem in Electrophotography* (Walter de Gruyter, Berlin, 1972), p. 287.
- ²K. Kinoshita, Japan Patent H5–19140 (1993) (in Japanese).
- ³ J. Decker, K. Fukae, S. Johnson, S. Kaieda, and I. Yoshida, *Proc. IS&T's NIP7: Int'l. Congress on Adv. in Non-Impact Printing Technologies* (IS&T, Springfield, VA, 1991) p. 328.
- ⁴K. Kubo, T. Kobayashi, S. Nagae, and T. Fujimoto, "Photoconduction Mechanism in Single-Layer Photoconductor with Metal-Free Phthalocyanine", J. Imaging Sci. Technol. **43**, 248–253 (1999).
- ⁵ A. Omote, Y. Itoh, and S. Tsuchiya, "Drift Mobility of Monolayer Photoreceptor with H₂-Phthalocyanine", J. Imaging Sci. Technol. **39**, 271 (1995).
- ⁶T. Kitamura, Y. Miyazawa, and H. Yoshimura, "Carrier Transport in Titanyl Phthalocyanine Pigment Dispersed in Binder Polymer", J. Imaging Sci. Technol. **40**, 171–175 (1996).
- ⁷Y. Hoshino, T. Murata, H. Watanabe, and I. Yoshida, "Surface Voltage Decay Model of Phthalocyanine Binder Type Photoreceptor", *Proc.*

- IS&T's NIP16: Int'l. Congress on Digital Printing Technologies (IS&T, Springfield, VA, 2000) pp. 129–132.
- ⁸ P. M. Borsenberger, A. Chowdry, D. C. Hoesterey, and W. Mey, "An aggregate organic photoconductor.II. Photoconduction properties", J. Appl. Phys. 49(11), 5555 (1978).
- ⁹ K. Seino and M. Yoshida, "Hysteresis Sensitization Effect in a CdSn•CdCO₃-Resin Dispersion-Type Photoreceptor", J. Imaging Sci. Technol. 36, 579–586 (1992).
- ¹⁰T. Kurita, *Proc. SEPJ* (The Society of Electrophotography of Japan, Tokyo, 1970) p. 7. (in Japanese).
- ¹¹S. M. Sze, *Physics of Semiconductor Devices*, 2nd ed. (John Wiley and Sons, New York, 1981), p. 255.
- ¹² H. A. Bethe, MIT Radiation Laboratory Report 43/12 (MIT, Cambridge, MA, 1942).
- ¹³ C. F. Hackett, "Characterization of an Active Matrix Binder Photoreceptor x-Form Metal-Free Phthalocyanine in Poly(*N*-vinyl Carbazole)", J. Chem. Phys. **55**, 3178 (1971).
- ¹⁴T. Konuma, H. Hirahara, I. Yoshida, and S. Kaieda, "Image Characteristics of High Gamma Single-Layer Photoreceptor", *Proc. ICJ Fall Meeting* (The Imaging Society of Japan, Tokyo, 2008) p. 57 (in Japanese).
- ¹⁵ P. M. Borsenberger and D. S. Weiss, Organic Photoreceptors for Xerography (Marcel Dekker Inc., New York, 1998), p. 55.